LA-7949-MS
Informal Report

Nondestructive Verification of Relative Burnup Values and Cooling Times of Irradiated MTR Fuel Elements

University of California

LOS ALAMOS SCIENTIFIC LABORATORY
Post Office Box 1663 Los Alamos, New Mexico 87545

LA-7949-MS
Informal Report
UC-78
Issued: August 1979

Nondestructive Verification of Relative Burnup Values and Cooling Times of Irradiated MTR Fuel Elements

J. R. Phillips
T. R. Bement
K. Kaieda*
E. G. Medina

*Visiting Scientist. Japan Atomic Energy Research Institute, Tokai-Mura, JAPAN.

NONDESTRUCTIVE VERIFICATION OF RELATIVE BURNUP VALUES AND COOLING TIMES OF IRRADIATED MTR FUEL ELEMENTS

by

J. R. Phillips, T. R. Bement, K. Kaieda, and E. G. Medina

ABSTRACT

Sixteen irradiated MTR fuel elements have been examined using nondestructive gamma-ray and neutron techniques. The consistency of declared burnup values and cooling times has been measured. Measured parameters have been identified that best predict the burnup and cooling time values of individual elements and their relative importances have been quantified using established statistical methods of analysis. Various detector systems, including germanium, cadmium telluride, and Be(γ,n) detector, and fission chamber have been used to measure the axial activity profiles.

I. INTRODUCTION

Nuclear power has been projected to supply a significant fraction of the total electricity output of the world by the year 2000.[1] Light-water reactors using low-enriched uranium (~3.5% ^{235}U) have generated more than 260 million megawatt days (MWD) of electrical energy over the past three decades.[2] A significant by-product of the fissioning process is the production of plutonium which can be used as fuel material for a nuclear explosives program. The accurate measurement and accountancy of the plutonium inventory of discharged light-water reactor fuels is an integral part of the total system of safeguards for the nuclear fuel cycle.

The Safeguards Technology Groups of the Los Alamos Scientific Laboratory have been actively investigating the problems associated with safeguarding irradiated fuels for the past two years. Many of the available nondestructive techniques and applications were reviewed as the background for an experimental

program.[3] Nondestructive gamma-ray and passive neutron techniques were selected as being the most applicable to the characterization of irradiated fuels. The plutonium inventory of an irradiated assembly cannot be measured directly using these techniques, therefore an indirect signature, that can be analytically related to the plutonium content, must be measured. Burnup is a measurable parameter that satisfies this condition. Burnup, defined as the integrated energy released from the fission of heavy nuclides initially present in the fuel, or as the percent of initial ^{235}U consumed, can be related directly to the remaining ^{235}U inventory as well as the plutonium produced. To determine the absolute burnup value of an individual fuel assembly independently of reactor history, the cooling time must be verified because the parameters measured are all time-dependent. The examination of an irradiated fuel assembly will usually occur after a significant time (½-5 yr) following discharge. Many of the gamma-ray and neutron signatures have half-lives of the same order as the cooling times, therefore the results must be corrected to obtain a consistent set of data.

Initially our investigations are primarily concerned with the development of gamma-ray and neutron techniques for burnup determination which involve also the determination of the cooling time. The original work was performed on highly-enriched Materials Test Reactor (MTR) fuel from the Omega West Reactor located at Los Alamos. The ease of access to the reactor as well as the ability to control the environment in which the examinations were performed provided a unique opportunity to test and evaluate techniques which could be applied to the characterization of Light Water Reactor (LWR) fuels at various reactor sites.

A. Previous Investigations

Several other gamma-ray examinations of irradiated MTR fuel assemblies have been performed. Dragnev et al concluded that the $^{144}Pr/^{137}Cs$ activity ratio was a suitable cooling time monitor for cooling times ranging from 0.5 to 5 years.[4] They obtained an average error of 4.6% for the measured cooling times when compared with the operator's declared values. The $^{134}Cs(796\ keV)/^{137}Cs(662\ keV)$ ratio with the correction for cooling times represented the burnup values with an average precision of 4.9%. Beets reported the use of the $^{95}Zr/Nb$ activity ratio as a convenient cooling time monitor for periods from several days up to one year, but better accuracy can be achieved from calibrated $^{95}Zr/^{137}Cs$ measurements.[5] The applications

of ^{137}Cs activity and $^{134}Cs/^{137}Cs$ activity ratio as burnup monitors were discussed with a relative precision of 9% for the $^{134}Cs/^{137}Cs$ results. These two investigations were based upon irradiated MTR fuel elements. Hanna recently published a rather complete evaluation of the experimental measurement of highly-enriched fuel elements for determination of cooling times and burnup values.[6,7] This work was compared with similar examinations performed by Dragnev.[4] The importance of neutron flux density during the irradiation of the assemblies was identified as one of the more critical parameters.

Other investigators have examined the application of nondestructive gamma-ray techniques for verification of burnup and cooling times in natural uranium fuels.[8,9] Valovic reported measuring burnup with a precision of 6% by comparing ^{137}Cs activities of the assemblies to a known reference assembly. Measurement of cooling times exhibited a 7-15% precision between declared and measured values.[9] An average difference of 2.2% between the $^{134}Cs/^{137}Cs$ analysis and the mass spectrometric results for 20 fuel elements was reported by Chen in the examination of CANDU fuels.[8] This report explored the possibility of calculating the integrated flux by relating calculated and measured $^{134}Cs/^{137}Cs$ ratios.

B. LASL Investigation

Sixteen irradiated MTR fuel elements with similar irradiation histories were measured nondestructively to evaluate which isotopic activities and/or isotopic ratios best explained the variation in cooling times and burnup. The declared cooling times ranged from 438 to 1456 days and the declared burnup values ranged from 27.44 to 33.48 atom percent. Axial scans were performed on four elements to investigate the correlation between the results obtained using rapid profile detectors and the results from the more detailed germanium data. These results have been applied to defining the critical parameters in the subsequent examinations of BWR and PWR fuels.

II. EXPERIMENTAL

The Omega West Reactor (OWR) is a 8-MW thermal, heterogeneous, tank-type research reactor which utilizes aluminum-clad fuel elements of the Materials Testing Reactor (MTR) type. The reactor core consists of a 4 x 9 array of fuel elements with each containing approximately 220 g of ^{235}U (93% enrichment). Each fuel element is constructed of 18 curved fuel plates, 1.52 mm (0.060 in.) thick mounted 2.97 mm (0.117 in.) apart in heavy aluminum side

plates. Each fuel plate contains a 61-cm (24 in.) long sheet of uranium-aluminum alloy that is sandwiched and hot rolled between two 0.51 mm (0.020 in.) thick sheets of pure aluminum.[10]

The sixteen irradiated elements examined during the two exercises are listed in Table I. Operator-declared burnup values range from 27.44 to 33.48 at. % (61.36 to 73.87g), with cooling times ranging from 438 to 1456 days. The specific burnup values were calculated from the irradiation history of the reactor and may have a significant error of approximately 5%. The reactor is operated as a research facility and has a very irregular operation history. A typical two-week reactor history is schematically presented in Fig. 1. During this period the reactor was only operated eight hours/day and at various power levels ranging from a relative minimum of 0.44 to a maximum of 1.0. This irregular operation introduced additional complications in the calculations of the theoretical activity levels of isotopes and isotopic ratios.

Four nondestructive techniques were investigated for the characterization of irradiated MTR fuels: gamma-ray techniques included the use of germanium detectors, cadmium telluride detectors and beryllium (γ,n) detectors; the neutron technique was based on the use of fission chambers.

There are two basic objectives in the examination of irradiated fuels for safeguards. The first is to determine the consistency of the relative burnup of individual fuel elements independently of any operator-supplied information and to determine if there are any values which lie outside specified limits (95% confidence bounds). This may be possible to accomplish by measuring the entire fuel element by gamma-ray and/or neutron methods which provide data that is correlated to the operator-declared burnup values. The second objective is the rapid measurement of the axial activity profile of the fuel elements. The axial profile measurement is essential to ensure that a segment of the fuel element has not been removed, thereby establishing the physical

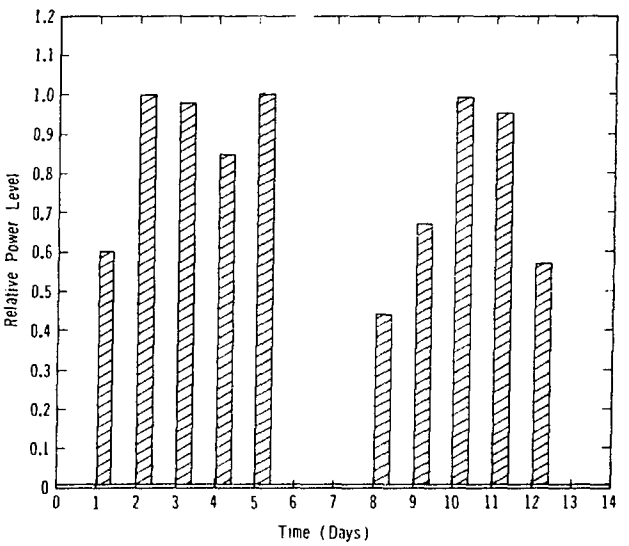

Fig. 1.
Two-week irradiation history of a fuel element in the Omega West Reactor.

TABLE I

MTR FUEL ELEMENTS NONDESTRUCTIVELY MEASURED

Fuel Element No.	Atom % Burnup	Grams Burnup	Discharge Date	Examination Dates	
E356	33.48	73.87	1/17/74	9/29/77	
E357	32.84	71.64	1/17/74		1/12/78
E359	31.62	69.46	4/8/74	9/28/77	1/11/78
E361	30.11	67.12	6/13/74	9/28/77	
E363	30.99	69.27	6/13/74	9/30/77	
E364	28.89	63.40	10/3/74	9/29/77	
E368	29.15	65.15	2/24/75	9/29/77	1/12/78
E370	27.74	61.36	4/21/75	9/29/77	1/13/78
E371	27.44	61.36	4/21/75	9/28/77	
E372	31.52	70.28	9/8/75	9/28/77	
E373	32.17	70.54	9/8/75		1/13/78
E374	29.47	65.65	11/1/77		1/13/78
E375	30.73	68.38	3/1/76		1/13/78
E378	29.29	65.37	3/22/76	9/28/77	
E379	29.78	66.22	3/22/76		1/13/78
E383	28.95	63.37	8/16/76		1/11/78

dimensions of the element. Also, if the relative burnup has been established at only one or a few points by more detailed analysis, the profile can be used as an integrating function to establish the integral burnup of the element.

The experimental apparatus is schematically represented in Fig. 2. The germanium detector was mounted on a moveable platform with a fan-shaped collimator attached. To obtain an axial scan of an irradiated fuel element, the detector-collimator assembly was translated along the principal axis. Complete gamma-ray spectra were recorded at specified axial positions and stored on magnetic media for future reference. A typical gamma-ray spectra with the major full-energy peaks identified is shown in Fig. 3. The extremely high gamma activity required the insertion of lead as an attenuator which explains the relatively flat energy spectra. Because only relative activities were being determined, the gamma-ray spectra were not corrected for differences in relative efficiencies as a function of gamma-ray energy.

The collimator was rotated 90 degrees permitting the entire fuel element to be examined for the measurements. This reduced the position sampling problem to a second order effect of geometry ($1/R^2$). That is, the effects of any anomalies in the axial profiles were reduced by examining the entire fuel element.

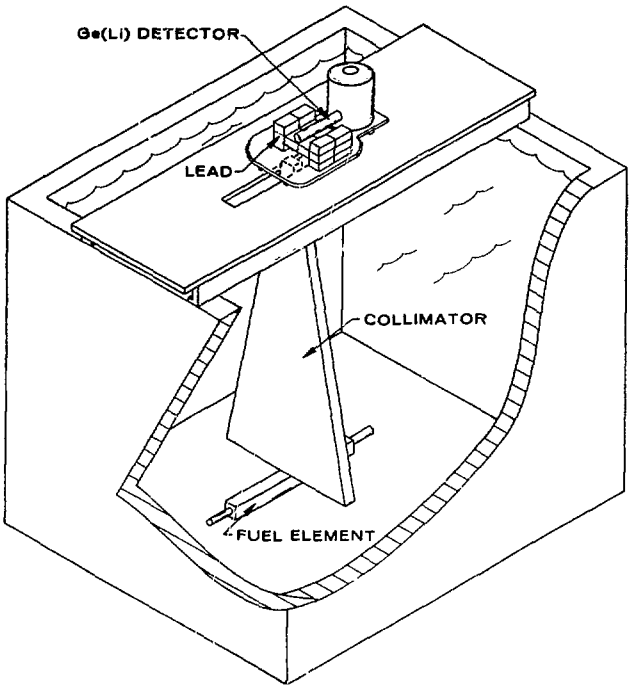

Fig. 2.
Germanium detector and collimator assembly for collection of integral gamma-ray spectra and isotopic axial profiles.

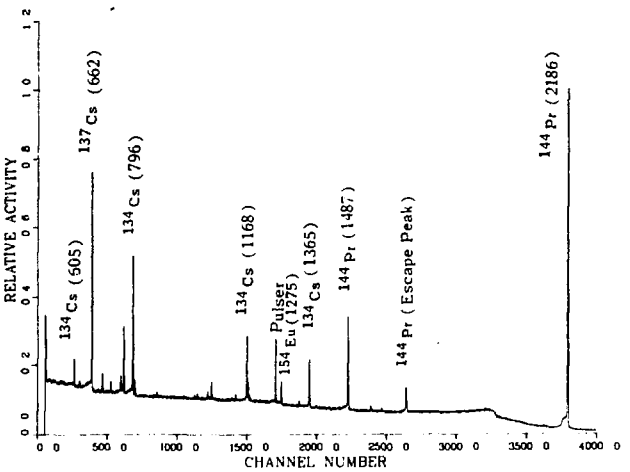

Fig. 3.
Typical gamma-ray spectra showing the principal full-energy peaks.

The procedure for the examination of an individual fuel element involved the transfer of the element from the reactor storage rack to an isolated examination pond 2.4 meters deep. Only one fuel element was in the pond at a time. All of the examinations were performed during a scheduled reactor maintenance period.

The axial profiles of four fuel elements were measured using the germanium detector system. Cadmium telluride detection of the gross gamma activities were recorded on two fuel elements. The higher-energy gross gamma activity profile was obtained using the beryllium (γ,n) detector. A high-energy gamma ray (2.186 MeV) can undergo an interaction with Be producing a neutron with an average energy of 510 keV[11] which after being moderated is detected using a ^{235}U fission chamber. A drawing of the Be(γ,n) detector in Fig. 4 shows the relative location of the principal components. The fission chamber was surrounded by a 4-cm thick polyethylene annulus to moderate the neutrons emitted

from the beryllium (Be) converter. Referring to the typical gamma-ray spectra (Fig. 3), the principal gamma-ray interacting with the Be and producing neutrons is the 2186-keV gamma ray of the fission product ^{144}Pr. The ^{144}Pr ($t_{1/2}$ = 17.28 m) is in secular equilibrium with its parent ^{144}Ce ($t_{1/2}$ = 284.4 d)[12], therefore, the axial profile obtained from this detector will represent the more recent irradiation exposure of the fuel element. The possible interference of spontaneous fission neutrons emitted from the fuel element was determined to be insignificant by removing the Be converter and measuring the fission chamber response. Spontaneous fission neutrons are primarily produced by the spontaneous fissioning of ^{242}Cm, ^{244}Cm and the even-numbered Pu isotopes. Since this fuel contained only 7% ^{238}U, the production of these transuranic isotopes should have been minimal.

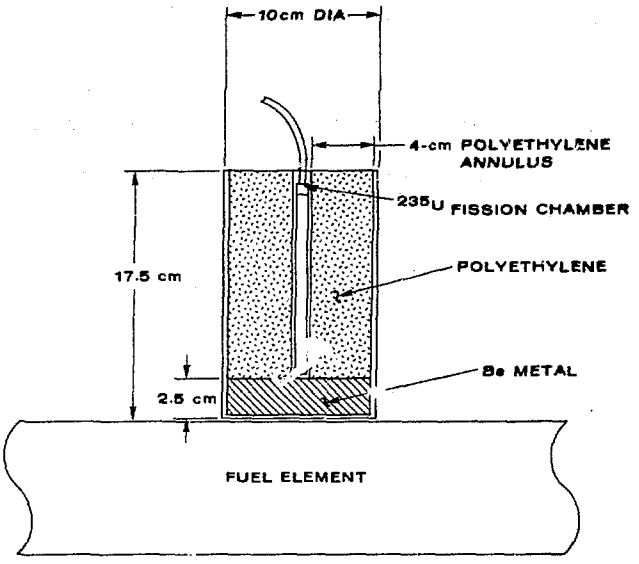

Fig. 4.
Beryllium (γ,n) detector for measuring the high-energy gamma-ray profile.

Various thicknesses (0.5, 1.0, 2.0, 3.0, and 4.0 cm) of the polyethylene annulus were evaluated prior to the selection of the 4-cm thick annulus for moderating the neutrons. Thicker discs of Be did not improve the efficiency of the detector assembly. The design of a Be(γ,n) detector was dependent upon the physical constraints and the specific fission chamber used to detect the neutrons.

A small cadmium telluride gamma detector was also used to monitor the axial gross gamma profiles of the irradiated fuel elements. The detector was placed in a small tube with a lead shield (first exercise) and a tungsten alloy shield (second exercise) to reduce the intense gamma field. In both cases, the shielding was insufficient to operate the CdTe in the pulse counting mode. The detector became saturated at any position closer than 80-cm to the fuel elements.

The relative neutron profile was measured with a large fission chamber with a 1.6 g loading of ^{235}U. This loading was forty times larger than the loading of the small fission chamber (38.6 mg ^{235}U) in the Be(γ,n) detector.

III. RESULTS

A. Statistical analyses for cooling time and burnup measurements

The objective of the analyses was to determine what variable or group of variables provided the best prediction of cooling time and burnup. The variables included specific activities of fission products, and ratios of activities. The criterion used to pick a predictor (or set of predictors) was the squared simple (or multiple) correlation coefficient (R^2). The quantity R^2 is expressed as

$$R^2 = \frac{(\hat{Y}_i - \bar{Y})^2}{(Y_i - \bar{Y})^2},$$

where $\hat{Y}_i$ is the ith observation, $\bar{Y}$ is the mean of the Y_i's and $\hat{Y}_i$ is the estimated value obtained from the regression equation. R^2 is the proportion of the total variation about the mean $\bar{Y}$ explained by the regression.[13] It is often expressed as a percentage by multiplying by 100. The R^2 value will be used throughout the remainder of the paper as a measure to quantify the degree of relationship between burnup or cooling time and measured variables.

A total of 33 gamma-ray peaks and isotopic ratios were considered as possible candidates for predictions. Consideration of all possible sets of predictions was impossible for two reasons. First, if all possible sets were considered, this would involve $2^{33}-1$ (or more than 8×10^9) separate linear regressions. Second, it was impossible or impractical to consider predictor sets containing large numbers of variables because of the limited amount of data available and because of the desire to keep the equations as simple as possible.

Several techniques were used to find predictor sets as nearly optimal as possible. Stepwise multiple regression[13] was used but a straightforward application of this procedure proved inadequate. Stepwise regression does not necessarily lead to maximum R^2 for a set of data. A greater problem was the fact that stepwise regression analysis resulted in the selection of different sets of predictors for the two exercises. Other multivariate data analysis procedures were used to reconcile these differences and to arrive at a set of predictors that did a good job in each exercise.

The motivation for using the multivariate techniques was to determine if the 33 predictor candidates could be divided into smaller groups on the basis of their information content. Such groupings could be useful for two reasons. One is to assure that variables containing information not present in any other variables are not arbitrarily excluded from consideration in the prediction equation. Secondly, if such groupings could be achieved, then it might not be necessary to use more than one variable from a group in a prediction equation. On the other hand, variables that do not fall in a well-defined group might have unique information to offer concerning the dependent variables. It is also possible that such predictor variables simply contain information which is contained in two or more of the other groups of variables.

The procedures used to examine the multivariate structure of the peaks and ratios were principal component analysis[14] and cluster analysis.[15,16] Principal component analysis was used to determine the number of dimensions required to contain most of the variation in the independent variables. Each dimension is a linear combination of the variables and is not necessarily a specific variable. If it is determined that most of the variation in the predictor variables is confined to a small number of dimensions, possibly two or three, it may be possible to separate these variables into groups with different information content. Ideally, one would like the information content of all groups to be mutually exclusive and exhaustive. This, however, can seldom, if ever, be achieved in practice.

Cluster analysis was used as an exploratory technique to search for groupings of the 33 predictor variables. From the principal component analysis we determined that most of the variation in the predictor variables was confined to a small number of dimensions, cluster analysis provided a qualitative method of grouping variables that would provide similar information. The selection of one variable from each grouping could provide sufficient information, whereby if we had selected two variables from a single grouping it is likely that we would not have significantly increased our total information about the set of data. Functionally we were attempting to obtain a relationship between a minimal number of measured variables and relative cooling times or burnups of individual assemblies. This can be illustrated by the following equation

$$\text{Cooling Time or Burnup} \propto f(C_1, C_2, C_3, \ldots) , \qquad (1)$$

where C_i is a variable from the ith cluster. A cluster can consist of a single variable and that would imply the variable could provide unique information with respect to the dependent variable (cooling time or burnup).

Several hierarchical clustering algorithms were applied to the 33 variables using the complement of the correlation coefficient (1-r) as a measure of the distance between variables. The furtherest neighbor (or complete linkage) algorithm was used as the primary means of separating the variables into groups. This algorithm has the property of exaggerating distance between variables. Some groupings were found which appeared in both exercises and these helped to resolve inconsistencies in stepwise regression results.

The statistical procedures described here were used to provide supplementary information for variable selection. They were not used with the intention of providing conclusive results and in fact, could not have done so with the relative small sample sizes available. They did, however, make it possible to look for patterns of relationship among a large number of variables which might otherwise escape one's attention.

B. Consistency of Relative Cooling Times

All of the gamma-ray and neutron signatures of irradiated fuel assemblies are functions of time-dependent variables. Therefore the measurements must be corrected for cooling times to permit the meaningful correlation between the declared and measured burnup values. Statistical analysis techniques were applied to the gamma-ray data to assist in the selection of specific variables for predicting the cooling times of individual fuel assemblies. In this investigation we assumed that the irradiation histories were similar for the set of fuel elements.

Cooling time can be expressed as the following:

$$t_c = -\frac{1}{\lambda_i} \ln \frac{A_i}{A_{oi}} \qquad \text{for a single isotope} \qquad (2)$$

and

$$t_c = \frac{1}{\lambda_j - \lambda_i} \ln \left[\frac{A_i}{A_j} \; \frac{A_{oj}}{A_{oi}} \right] \qquad (3)$$

for the ratio of two isotopes with λ_i the decay constant, A_i, the measured isotopic activity at time t_c, and A_{oi} the activity of the ith isotope at $t_c = 0$ (or end of irradiation). A_o will be a function of the reactor history which is in reality a time-dependent function. Both of the above functions for t_c can be approximated by a linear function when t_c and $(\lambda_j-\lambda_i)t_c$ are small values.

For the relationship of two activities, there are two general classifications of isotopes. The first group consists of ratios with both isotopes being a direct fission product and therefore directly proportional to the integrated flux (assuming the absorption cross-section is small). The isotopes in this group consist of ^{137}Cs ($t_{\frac{1}{2}}$ = 30.12 yr), ^{144}Ce-^{144}Pr ($t_{\frac{1}{2}}$ = 284.4 days), and ^{106}Ru-^{106}Rh ($t_{\frac{1}{2}}$=369 days) which were measureable in the spectra we obtained from this set of assemblies. The second group consists of ^{134}Cs($t_{\frac{1}{2}}$ = 2.06 yr) and ^{154}Eu ($t_{\frac{1}{2}}$ = 8.6 yr) which results from the (n,γ) reaction on the fission products ^{133}Cs and ^{153}Eu, respectively. In these cases

$$t_c = \frac{1}{\lambda_2-\lambda_1} \ln \frac{A_1}{A_2} + f(\phi,\beta), \qquad (4)$$

where A_1 is proportional to ϕ^β with $1 < \beta \leq 2$ and A_2 is proportional to ϕ. The $f(\phi,\beta)$ is a function of the integrated flux and the exponent β. The functional relationship of β with respect to the integrated flux (or burnup) of various elements will be discussed in the section on the axial measurements.

Two basic approaches to the solution of the relationship of measured gamma-ray activities with declared cooling times were investigated. (1) The first model used known coefficients for $1/\lambda$ and $1/(\lambda_2-\lambda_1)$ and solved for the average $\ln A_o$ and $\ln(A_{o2}/A_{o1})$ values. These averages were then used in place of the individual values in expressing the relationship between activity and cooling time. (2) The second model was a simple linear relationship between cooling time and activity at time, t_c. Each technique requires assumptions that can limit its applicability under certain circumstances. Each approach will be discussed in detail in the following subsections.

1. Model Using Known Decay Constants. In this section we assume that the following relationship is true for individual isotopes

$$A_i = A_{oi}\, e^{-\lambda_i t_c} \tag{5}$$

or

$$t_c = \frac{1}{\lambda_i} \ln A_{oi} - \frac{1}{\lambda_i} \ln A_i \tag{6}$$

where A_i = measured activity of the ith isotope after cooling time, t_c
A_{oi} = actual activity of the ith isotope at the end of irradiation
λ_i = decay constant of ith isotope
t_c = cooling time.

For isotopic ratios where each isotope is proportional to the integrated flux, ϕ, or each isotope is proportional to $\phi^{\beta i}$ where $1 < \beta_i < 2$ and β_i is not significantly different from β_j, the following is true

$$t_c = \frac{1}{\lambda_2-\lambda_1} \ln\left(\frac{A_1}{A_2}\right) + \frac{1}{\lambda_2-\lambda_1} \ln\left(\frac{A_{o2}}{A_{o1}}\right) . \tag{7}$$

Note that neither equation includes any error term. Therefore all the variability must be attributed to (A_{oi}) and (A_{o2}/A_{o1}) for the single isotope and the ratio variables. Since A_{oi} and (A_{o2}/A_{o1}) are unknown and cannot be determined without knowledge of t_c the values $(\ln A_{o2})$ and $\ln(A_{o1}/A_{o2})$ have to be estimated based upon the data that is available. Therefore the estimate of t_c based upon a single isotope is

$$\hat{t}_c = \frac{1}{\lambda}\left[\overline{\ln A_o} - \ln A_i\right], \tag{8}$$

where $\overline{\ln A_o}$ is the average $\ln A_o$ value determined from the set of assemblies examined. Similarly, for the ratio data, the following relationship is true

$$\hat{t}_c = \frac{1}{\lambda_2-\lambda_1}\left[\overline{\ln\left(\frac{A_{o2}}{A_{o1}}\right)} + \ln\left(\frac{A_1}{A_2}\right)\right] . \tag{9}$$

For the single isotopes the ^{134}Cs(605 keV), ^{106}Rh(1050 keV), and ^{144}Pr(1487 keV) activities provided the most consistent data related to cooling times as shown in Table II. The average differences for these single isotopes ranged from 5.1% to 10.7%. The results for the best four isotopic ratios are given in Table III with the average scatter in the values ranging from 2.7% to 7.8%. These differences corresponded to errors as large as one hundred days which can result in over a 30% error in correcting the measured activity to the activity at discharge for isotopes with half-lives of 300 days (^{144}Ce-^{144}Pr; $t_{\frac{1}{2}}$=284.4 days) and (^{106}Ru-^{106}Rh; $t_{\frac{1}{2}}$=369 days).

To obtain an estimate of the variance of the difference between $\hat{t}_c$ and the true t_c for a particular element we can calculate the following if we assume $\overline{\ln A_o}$ and $\ln A_i$ are independent for the single isotope.

$$\mathrm{Var}(\hat{t}_c - t_c) = \frac{1}{\lambda}\left[\mathrm{Var}(\ln A_o)(1 + 1/N) + \mathrm{Var}(\ln A)\right] . \qquad (10)$$

Making similar assumptions for the ratio of two isotopes

$$\mathrm{Var}(\hat{t}_c - t_c) = \left(\frac{1}{\lambda_2 - \lambda_1}\right)^2 \left[\mathrm{Var}\left(\ln \frac{A_{o2}}{A_{o1}}\right)(1 + 1/N) + \mathrm{Var}\left(\ln \frac{A_1}{A_2}\right)\right]. \qquad (11)$$

The assumptions of independence are reasonable if the element in question were not used to compute $\overline{\ln A_o}$.

In each of the above cases it can be seen that the variance of $(\hat{t}_c - t_c)$ is composed of two parts; the first due to using the average log discharge activity to estimate the actual discharge activity and the second due to variation in activities at time t_c. It can be shown that for data similar to that reported here, the first source of variation is the major contributor to $\mathrm{Var}(\hat{t}_c - t_c)$. In Table IV the standard deviation of $(\hat{t}_c - t_c)$ (the square root of the variance) is listed for the best single isotopes and for the best ratios. Values of $\mathrm{Var}(\overline{\ln A_o})$, $\mathrm{Var}(\ln A)$, $\mathrm{Var}[\overline{\ln(A_{02}/A_{01})}]$, and $\mathrm{Var}[\ln(A_{o1}/A_{o2})]$ typical of those found in this exercise were used to generate the table.

TABLE II

COMPARISON OF THE CONSISTENCY OF ESTIMATED COOLING TIMES - SINGLE ISOTOPES - MODEL (1)

Elements

September Data	E356	E359	E361	E363	E364	E368	E370	E371	E372	E378	Average Difference
Declared Values (Days)	1350	1268	1202	1204	1091	947	891	890	750	554	
Values Based on Regression Equation											
^{134}Cs	1211	1162	1221	1151	1185	1007	1078	910	748	492	7.4%
^{106}Rh	1187	1117	1183	1186	1138	1008	966	967	802	612	7.2%
^{144}Pr	1229	1204	1171	1177	1115	1017	946	934	781	593	5.1%

Elements

January Data	E357	E359	E368	E370	E373	E375	E379	Average Difference
Declared Values (Days)	1456	1374	1053	998	858	683	662	
Values Based on Regression Equation								
^{134}Cs	1294	1292	1242	1090	723	721	726	10.7%
^{106}Rh	1274	1278	1107	1040	906	774	709	7.8%
^{144}Pr	1328	1302	1103	1022	869	761	703	5.7%

TABLE III

COMPARISON OF THE CONSISTENCY OF ESTIMATED COOLING TIMES - ISOTOPIC RATIOS - MODEL (1)

Elements

September Data	E356	E359	E361	E363	E364	E368	E370	E371	E372	E378	Average Difference
Declared Values (Days)	1350	1268	1202	1204	1091	947	891	890	750	554	
Values Based on Regression Equation											
$^{144}Pr/^{137}Cs$	1324	1286	1221	1232	1124	988	893	891	715	491	3.1%
$^{134}Cs/^{154}Eu$	1414	1276	1175	1050	1114	784	993	907	950	503	7.8%
$^{106}Rh/^{137}Cs$	1304	1193	1261	1270	1163	961	900	921	718	474	5.1%
$^{106}Rh/^{144}Pr$	1370	1497	1130	1146	1036	1049	877	822	709	529	5.6%

Elements

January Data	E357	E359	E368	E370	E373	E375	E379	Average Difference
Declared Values (Days)	1456	1374	1053	998	858	683	662	
Values Based on Regression Equation								
$^{144}Pr/^{137}Cs$	1463	1404	1095	995	863	681	587	2.7%
$^{134}Cs/^{154}Eu$	1443	1349	1136	937	813	688	723	4.5%
$^{106}Rh/^{137}Cs$	1441	1414	1097	1011	917	664	545	5.3%
$^{106}Rh/^{144}Pr$	1514	1382	1090	960	742	718	682	4.8%

TABLE IV

STANDARD DEVIATIONS OF $(\hat{t}_c - t_c)$ BY USING THE AVERAGE $\ln(A_o)$ and $\ln(A_{o2}/A_{o1})$ VALUES

Isotope	Number of Samples in Set	Standard Deviation of $(\hat{t}_c - t_c)$
^{134}Cs(605 keV)	10	± 114 days
	5	± 133 days
^{106}Rh(1050 keV)	10	± 110 days
	5	± 129 days
^{144}Pr(1487 keV)	10	± 74 days
	5	± 86 days
Ratio		
$^{144}Pr/^{137}Cs$	10	± 41 days
	5	± 48 days
$^{134}Cs/^{154}Eu$	10	± 82 days
	5	± 94 days
$^{106}Rh/^{137}Cs$	10	± 60 days
	5	± 69 days
$^{106}Rh/^{144}Pr$	10	± 99 days
	5	± 114 days

2. Linear Model

This model relates the cooling times with the measured isotopic activities and ratios with

$$t_c = a + b(A_i \text{ or } A_i/A_j) \quad , \tag{12}$$

where t_c was the cooling time, A_i and A_i/A_j were the measured activities of the ith and jth isotopes, and a and b were the parameters of the regression equation. As was discussed earlier this relationship can be a good approximation when λt_c and $(\lambda_1 - \lambda_2)t_c$ are small. This model is the simplest of the two models discussed and is easy to apply provided the above conditions can be assumed to exist.

Principal component analysis indicated that over 86% of the variation in the September data was confined to a two-dimensional space. By increasing the dimensions to three, 94% of the variation was explained. In the January data more than 95% of the variation in the predictor variable is confined to a two-dimensional space. From these analyses there appear to be two or three independent sources of variations in the data. Based upon this we would hope to find two or three relatively independent groups of predictor variables among the set of 33 variables that contain most of the available information concerning cooling time.

Cluster analysis was used as an exploratory technique to see if there were subgroups of variables that appeared in both September and January data sets. For both the September and January data four distinct groups of variables appeared in the set of 33 variables. The four clusters are listed in Table V. The ^{134}Cs (605 keV)/^{137}Cs (662 keV) (Cluster I) and the ^{154}Eu (1275 keV)/^{144}Pr (2186 keV) (Cluster IV) isotopic ratios seemed to do a very good job of explaining cooling time variation in both exercises.

The ^{134}Cs (605 keV)/^{137}Cs (662 keV) isotopic ratio explained 91.4% of the variation in cooling times for the September data (Fig. 5) and 92.9% for the January data (Fig. 6). On each of the plots, the 95% confidence bounds are shown. These bounds may be interpreted as defining a region within which one is 95% confident that the individual cooling time value will fall for a measured ratio value. The width of these bounds depends upon several factors. Two factors that cannot be controlled by the experimenter are the values of the ratio at which one wishes to estimate the cooling time and the values of the standard deviations of cooling time for a fixed ratio (the bounds become wider as this quantity increases). Two other factors that can be controlled by the experimenter to some extent are the spread of the ratio values used in the least-squares analysis and the number of elements used. The width of the confidence bounds decreases as either the spread of ratios or number of elements used increases.

Similarly, the values for the ^{154}Eu (1275 keV)/^{144}Pr (2186 keV) explained 95.5% and 96.8% of the variations for the September data (Fig. 7) and January data (Fig. 8), respectively. Table VI shows these results for individual fuel elements, plus the results of a linear combination of these two ratios which explained over 99% of the variations in each of the data sets. The January results have been calculated twice: once with element E374

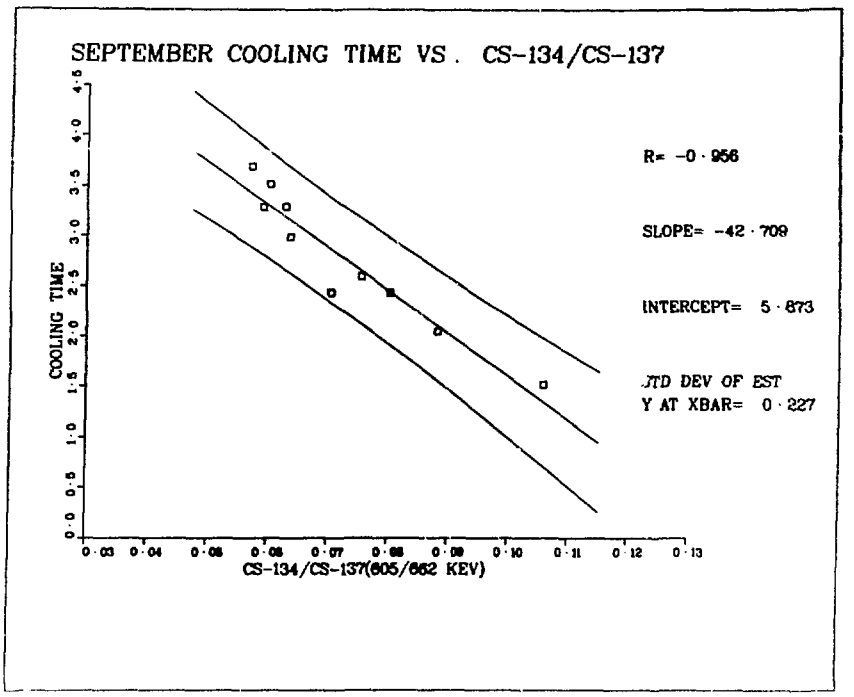

Fig. 5.
Plot of cooling time in years versus the $^{134}Cs(605\ keV)/^{137}Cs(662\ keV)$ isotopic ratio for the September data.

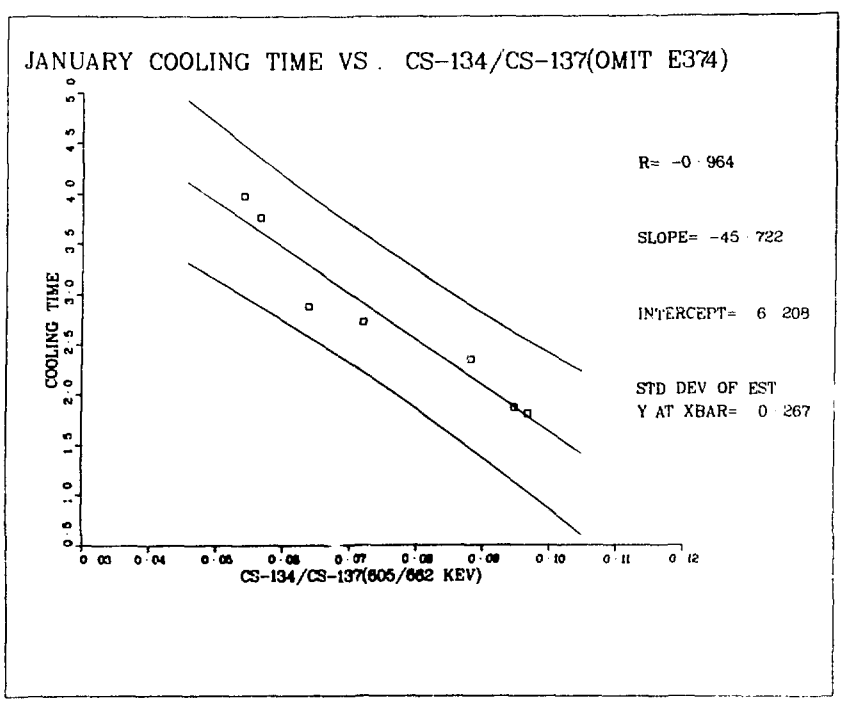

Fig. 6.
The cooling time with respect to the $^{134}Cs(605\ keV)/^{137}Cs(662\ keV)$ isotopic ratio is shown for the January data.

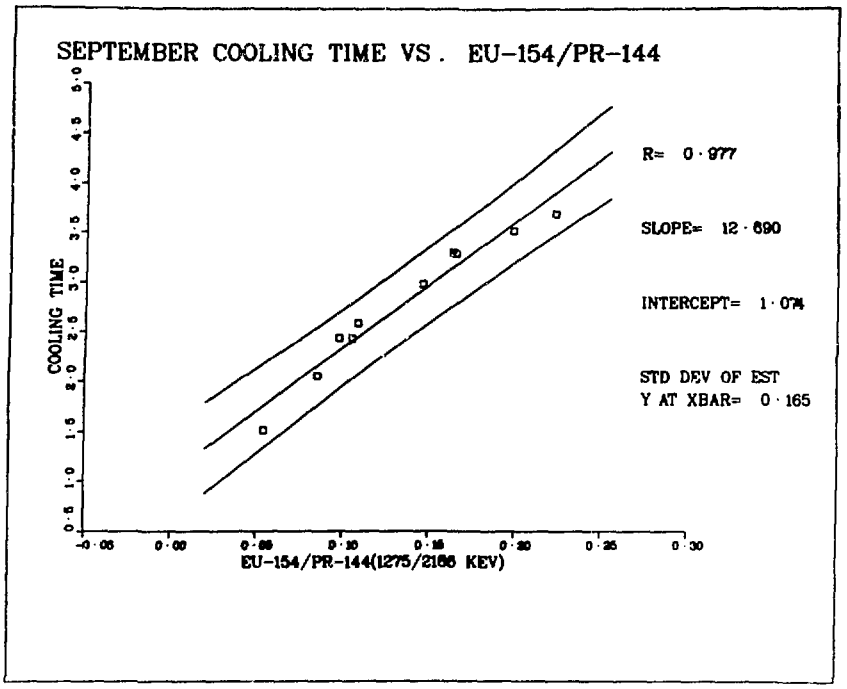

Fig. 7.
Linear least squares fit of cooling time with respect to the ^{154}Eu(1275 keV)/ ^{144}Pr(2186 keV) isotopic ratios for the September data.

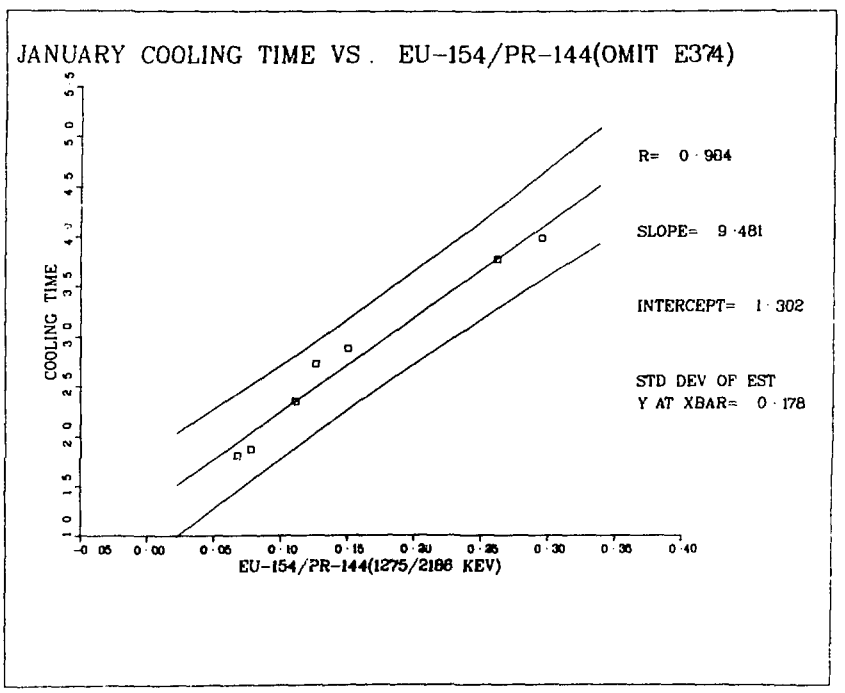

Fig. 8.
Linear least squares fit of cooling time with respect to the ^{154}Eu(1275 keV)/ ^{144}Pr(2186 keV) isotopic ratios for the January data.

TABLE V

CLUSTERS FOR SELECTION OF COOLING TIME VARIABLES - MODEL (2)

Cluster I	Cluster II	Cluster III	Cluster IV
^{134}Cs(605 keV)	^{137}Cs(662 keV)	^{154}Eu(1005 keV)	$^{134}Cs(605)/^{144}Pr(696)$
^{134}Cs(796 keV)		^{154}Eu(1275 keV)	$^{134}Cs(796)/^{144}Pr(696)$
^{134}Cs(1038 keV)		$^{154}Eu(1275)/^{137}Cs(662)$	$^{134}Cs(796)/^{144}Pr(2186)$
^{134}Cs(1365 keV)			$^{134}Cs(1365)/^{144}Pr(2186)$
$^{134}Cs(605)/^{137}Cs(662)$			$^{134}Cs(796)/^{106}Rh(1050)$
$^{134}Cs(796)/^{137}Cs(662)$			$^{154}Eu(1005)/^{106}Rh(1050)$
$^{134}Cs(1038)/^{137}Cs(662)$			$^{154}Eu(1275)/^{106}Rh(1050)$
$^{134}Cs(1365)/^{137}Cs(662)$			$^{154}Eu(1005)/^{144}Pr(1487)$
^{106}Rh(1050 keV)			$^{154}Eu(1275)/^{144}Pr(1487)$
^{144}Pr(696 keV)			$^{154}Eu(1275)/^{144}Pr(2186)$
^{144}Pr(1487 keV)			
^{144}Pr(2186 keV)			

included in the data and once without. All of the elements had irregular irradiation exposures as indicated by Fig. 1, however, the history of E374 was very different from the other elements. It was irradiated for 707 days, then removed from the core and allowed to cool for 313 days. It was then reirradiated for another 246 days. Therefore, the January results presented in Table VI do not include the E374 element in the analysis.

Comparison of the Two Models for Estimating Relative Cooling Times

In both of the models evaluated various assumptions have to be accepted prior to their application to the fuel assemblies examined. We have assumed that each fuel assembly has been exposed to a similar irradiation history. This assumption is critical in each of the models. As discussed in the last two sections this was illustrated by including the results for element E374 which had a significantly different irradiation history.

TABLE VI

COOLING TIME RESULTS BASED ON $^{134}Cs/^{137}Cs$ AND $^{154}Eu/^{144}Pr$ RATIOS - MODEL (2)

	Elements											
September Data	E356	E359	E361	E363	E364	E368	E370	E371	E372	E378	% Variation Explained	Average Difference
Declared Values (Days)	1350	1268	1202	1204	1091	947	891	890	750	554		
Values Based on Regression Equation												
$^{134}Cs/^{137}Cs$	1254	1206	1222	1165	1153	968	1045	892	770	492	91.4	5.6%
$^{154}Eu/^{144}Pr$	1428	1313	1158	1150	1070	895	843	879	787	643	95.5	5.3%
$\left[^{134}Cs/^{137}Cs\right] + \left[^{154}Eu/^{144}Pr\right]$	1376	1284	1194	1165	1110	920	922	877	766	555	99.2	
Percent Difference	+1.9	+1.3	-0.7	-3.2	+1.7	-5.7	+3.5	-0.3	+2.1	+0.2		2.1%

	Elements										
January Data	E357	E359	E368	E370	E373	E374[1]	E375	E379			Average Difference
Declared Values (Days)	1456	1374	1053	998	858	438	683	662			
Values Based on Regression Equation[2]											
$^{134}Cs/^{137}Cs$	1366	1324	1202	1065	795	470	686	651		92.9	5.7%
$^{154}Eu/^{144}Pr$	1534	1413	1013	927	873	565	753	717		96.8	5.6%
$\left[^{134}Cs/^{137}Cs\right] + \left[^{154}Eu/^{144}Pr\right]$	1466	1373	1078	970	826	496	708	672		99.5	
Percent Difference	+0.7	-0.1	+2.4	-2.8	-3.7	+11.7	+3.7	+1.5			2.1%

[1] E374 was irradiated for 707 days, then cooled for 313 days before being irradiated another 246 days. This result was declared an outlier and was not included in the remaining analysis.

[2] Values computed from data set excluding E374.

Either the nonlinear or the linear model can be used to predict the consistency of relative cooling times with a precision of 1 to 6 relative percent. The nonlinear model (1) generally gives slightly better predictions than the linear model because the required condition that λt_c and $(\lambda_1 - \lambda_2)t_c$ must be small is not satisfied for all assemblies. For the cooling times we examined, the ^{144}Pr isotope appears as the best single isotope predictor as well as being a component of most of the ratios and linear combinations. This may be explained by two reasons. First, the half-life of ^{144}Pr(284.4d) is comparable to the cooling times of these sets of fuel assemblies, and secondly, the two gamma-ray peaks at 1487 and 2186 keV were measured very precisely because of their relative activities.

In applying either of these models, the experimenter must be cautious because of the effect that irradiation histories can have upon the results. This is particularly true when ^{134}Cs and ^{154}Eu occur in the ratios which predict the cooling times in both the nonlinear and linear models. Both of these isotopes can be produced by one or more neutron captures of the fission products which are very dependent upon irradiation precursor histories. The contribution of ^{134}Cs and ^{154}Eu should be a function of the integrated flux that the assemblies had been exposed to during irradiation. The functional relationship of these two isotopes with respect to the flux will be discussed further in the section on Axial Profile Measurements.

IV. BURNUP MEASUREMENTS

The gamma-ray results for the fission products were corrected for the declared cooling time, and then analyzed to determine which variable or set of variables provided the best prediction of burnup values. All of the burnup calculations were based upon the total number of grams ^{235}U fissioned. Because of the experimental arrangement, the entire fuel element was examined. The initial ^{235}U loading of individual fuel elements varied from 218 to 224 grams, and the operator-declared grams of ^{235}U fissioned ranged from 61 to 74 grams.

Principal component analysis showed that in the September data over 79% of the variation in the predictor variables was confined to a two-dimensional space. By increasing the dimensions to three, almost 88% of the variation was explained. However, over 92% of the variation in the January data was confined to a two-dimensional space. There appears to be considerably more variation in

the September data than in the January data. Perhaps for this reason, fewer variables could be identified as falling in well-defined groups in both exercises. Table VII shows three groups that did appear in each exercise. The ^{154}Eu (1275 keV)/^{144}Pr (2186 keV) and ^{134}Cs (796 keV)/^{137}Cs (662 keV) isotopic ratios and ^{137}Cs (662 keV) did not fall in any specific groups that were identifiable in both the September and January exercises. Four variables, ^{137}Cs (662 keV), ^{134}Cs (605 keV)/^{137}Cs (662 keV), ^{134}Cs (796 keV)/ ^{137}Cs (662 keV), and ^{154}Eu (1275 keV)/^{137}Cs (662 keV) were determined to be among the most important predictors of relative burnup values, when considering both exercises.

The measured results for the relative burnup values are shown in Table VIII in which the September and January data are separated. In each exercise the burnup results were computed based upon the ^{137}Cs (662 keV), ^{134}Cs (605 keV)/^{137}Cs (662 keV), ^{134}Cs (796 keV)/^{137}Cs (662 keV), and ^{154}Eu (1275 keV)/^{137}Cs (662 keV) values. Of these four values, the ^{137}Cs (796 keV)/^{137}Cs (662 keV) ratio explained most of the variation (70.4%) in the September exercise. The best two variable linear combinations (72.4% of

---

TABLE VII

GROUPS OF PREDICTORS OF BURNUP FOR DATA CORRECTED FOR COOLING TIME

Cluster I	Cluster II	Cluster III
$^{134}Cs(605)/^{144}Pr(696)$	$^{134}Cs(605$ keV)	$^{106}Rh(1050$ keV)
$^{134}Cs(796)/^{144}Pr(696)$	$^{134}Cs(605)/^{137}Cs(662)$	$^{144}Pr(1487$ keV)
$^{134}Cs(796)/^{144}Pr(2186)$		$^{144}Pr(2186$ keV)
$^{134}Cs(1365)/^{144}Pr(2186)$		
$^{134}Cs(796)/^{106}Rh(1050)$		
$^{134}Cs(1038)/^{106}Rh(1050)$		
$^{154}Eu(1005)/^{144}Pr(1487)$		
$^{154}Eu(1275)/^{144}Pr(1487)$		
$^{154}Eu(1275)/^{144}Pr(2186)$		
$^{154}Eu(1275)/^{106}Rh(1050)$		

TABLE VIII

CONSISTENCY OF CALCULATED BURNUP VALUES BASED UPON DECLARED COOLING TIMES

	Element Identification											
September Data	E356	E359	E361	E363	E364	E368	E370	E371	E372	E378	% Variation Explained	Average Difference
Declared Values [3]	73.87	69.46	67.12	69.27	63.40	65.15	61.36	61.36	70.28	65.37		
Values Based on Regression Equation												
$^{137}Cs(662)$	70.84	70.03	66.98	67.28	63.85	62.76	62.68	64.33	67.54	70.37	58.5	3.1%
$^{134}Cs(605)/^{137}Cs(662)$	73.54	70.26	65.36	68.57	64.18	66.69	60.84	67.41	65.96	66.81	49.3	2.8%
$^{134}Cs(796)/^{137}Cs(662)$	73.52	70.51	65.99	65.49	64.40	62.39	64.21	64.54	69.46	66.05	70.4	2.7%
$^{154}Eu(1275)/^{137}Cs(662)$	69.80	68.18	65.28	64.64	65.66	63.62	65.39	67.45	70.60	65.99	30.8	4.0%
$^{137}Cs(662)$ + $^{134}Cs(796)/^{137}Cs(662)$	73.21	70.65	66.23	65.95	64.01	62.14	63.50	64.28	69.06	67.36	72.4	2.7%
Percent Difference	-0.9	+1.6	-1.3	-4.8	+0.9	-4.6	+3.5	+4.8	-1.7	+3.0		

	Element Identification									
January Data	E357	E359	E368	E370	E373	E374[1]	E375	E379		Average Difference
Declared Values	71.64	69.46	65.15	61.36	70.54	65.65	68.38	66.22		
Values Based on Regression Equation[2]										
$^{137}Cs(662)$	71.56	69.68	63.79	64.58	71.45	66.44	66.98	65.52	86.9	1.7%
$^{134}Cs(605)/^{137}Cs(662)$	70.86	69.67	63.24	66.20	69.7[illegible]	63.28	66.34	66.49	57.3	2.5%
$^{134}Cs(796)/^{137}Cs(662)$	71.75	69.79	64.31	64.83	67.[illegible]3	63.34	66.22	68.37	56.3	2.8%
$^{154}Eu(1275)/^{137}Cs(662)$	71.50	69.20	64.27	62.86	69.21	62.93	66.40	69.25	76.4	2.6%
$^{137}Cs(662)$ + $^{154}Eu(1275)/^{137}Cs(662)$	71.95	69.66	63.65	63.39	70.72	64.92	66.63	67.21	86.1	1.5%
Percent Difference	+0.4	+0.3	-2.3	+3.3	+0.3	-1.1	-2.6	+1.5		

[1] Element E374 results are based upon the data including E374 data in analysis.

[2] Measured values are based upon seven elements, with E374 excluded because of irregular irradiation exposure.

[3] Burnup values are expressed in grams ^{235}U.

the variation) for September were the ^{137}Cs (662 keV) and ^{134}Cs (796 keV)/^{137}Cs (662 keV) with the $^{134}Cs/^{137}Cs$ being the dominant term. An average absolute percentage difference of 2.7% between the declared and predicted values was obtained in this data set. By increasing the number input parameters to include all four measured values, the percent variation explained increased from 72.4% to 80.3%. Plots of these four parameters versus the declared burnup values are presented in Figs. 9-12 with the 95% confidence bounds plotted. The qualifying statements discussed in the cooling time results section are also applicable to these results.

The results for the January data (Figs. 13-16) are presented in Table VIII and are similar to those obtained in the September exercise except that the linear combination of ^{137}Cs (662 keV) and ^{154}Eu (1275)/^{137}Cs (662) provided the best correlations. Both the ^{137}Cs (662 keV) by itself and the linear combination explained about 86% of the variations in the declared burnup values. The results for element E374 were excluded because of its irregular irradiation history (discussed in the section on cooling times). In this particular exercise there is not any advantage in extending the analysis to include more than two variables. However, if all four variables are included, the percent variation explained significantly increases to 94.3% (Table IX).

There are three basic assumptions necessary in evaluating the results using the above analysis techniques. First, the relationship between the isotopic ratios and grams of ^{235}U burnup is linear. This allows the estimation of error based on the deviations from a straight-line fit. Second, the distribution of deviations about the straight line is assumed to be Gaussian with zero mean and constant standard deviation. Third, the variance of the measured ratios due to the measuring statistics are insignificant.

The agreement between the predicted values and the declared values for the burnup of individual assemblies was very good. However, these correlations demonstrate a consistency between the two values and still require some irradiation history information to allow the independent verification of the declared burnup values.

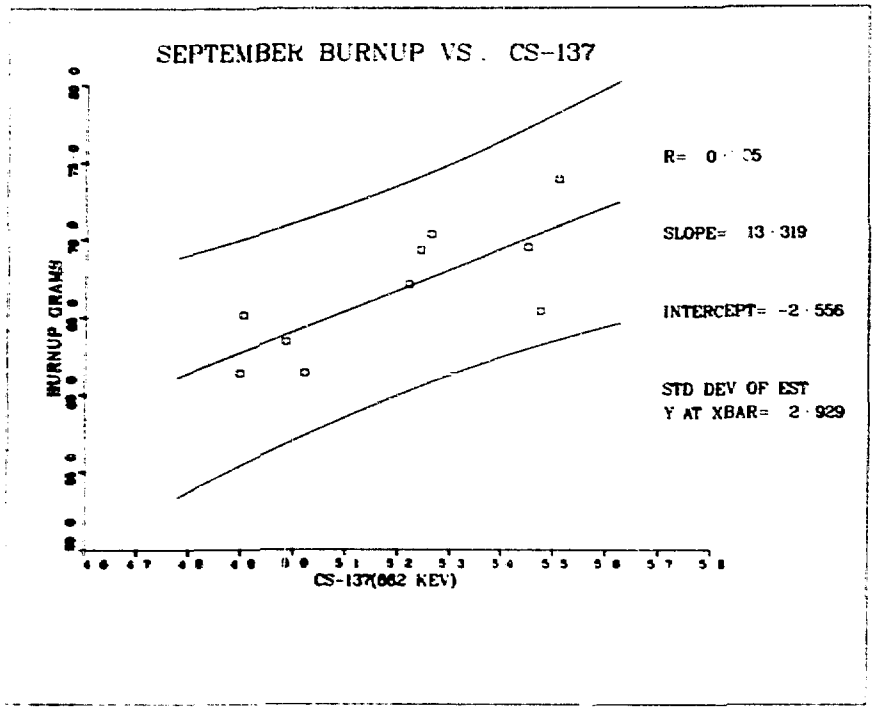

Fig. 9.

The linear relationship of declared burnup in grams with respect to ^{137}Cs (662 keV) activity for the September data.

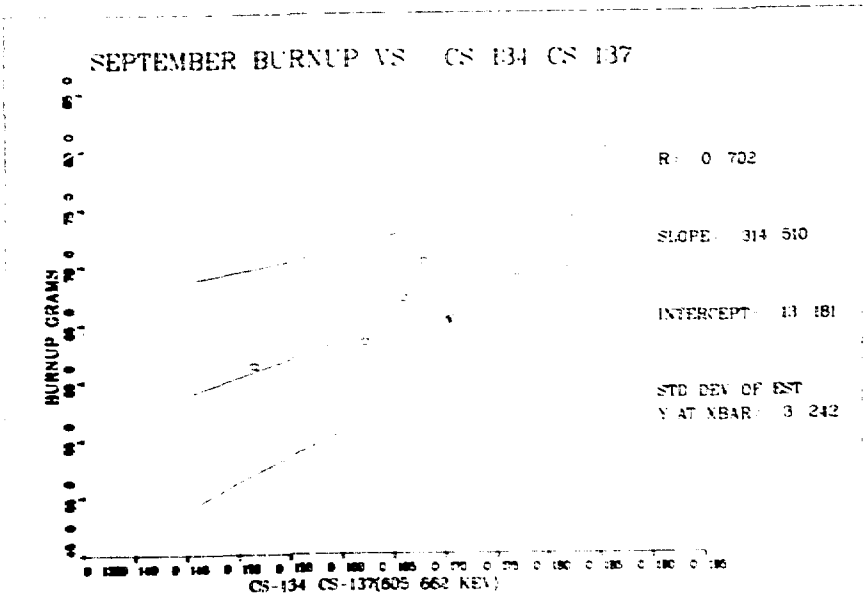

Fig. 10.

The linear relationship of declared burnup in grams with respect to ^{134}Cs (605 keV)/^{137}Cs(662 keV) isotopic ratio.

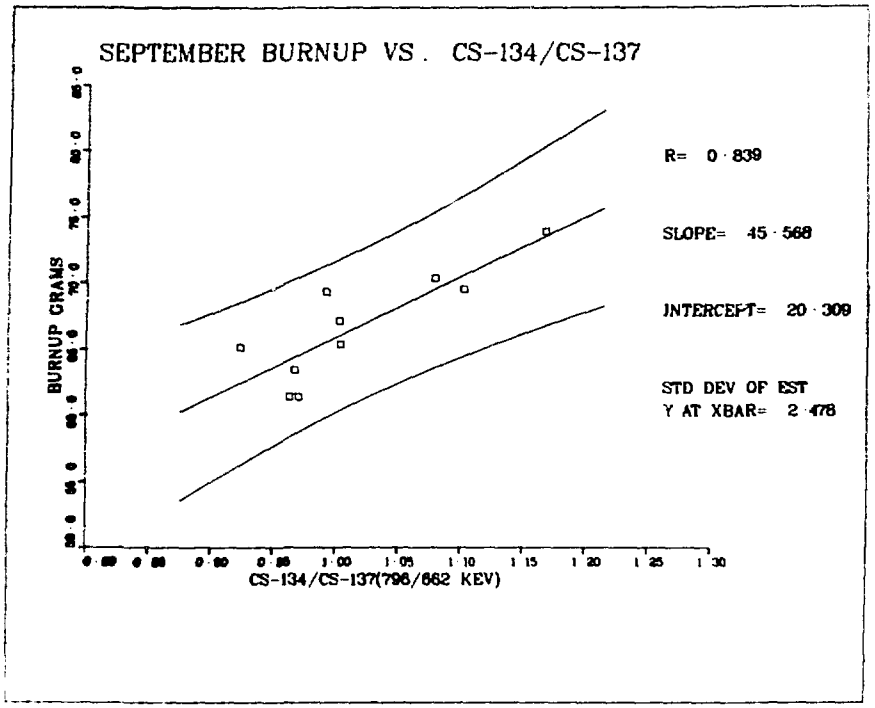

Fig. 11.

The linear relationship of declared burnup in grams with respect to ^{134}Cs (796keV)/^{137}Cs(662 keV) isotopic ratio.

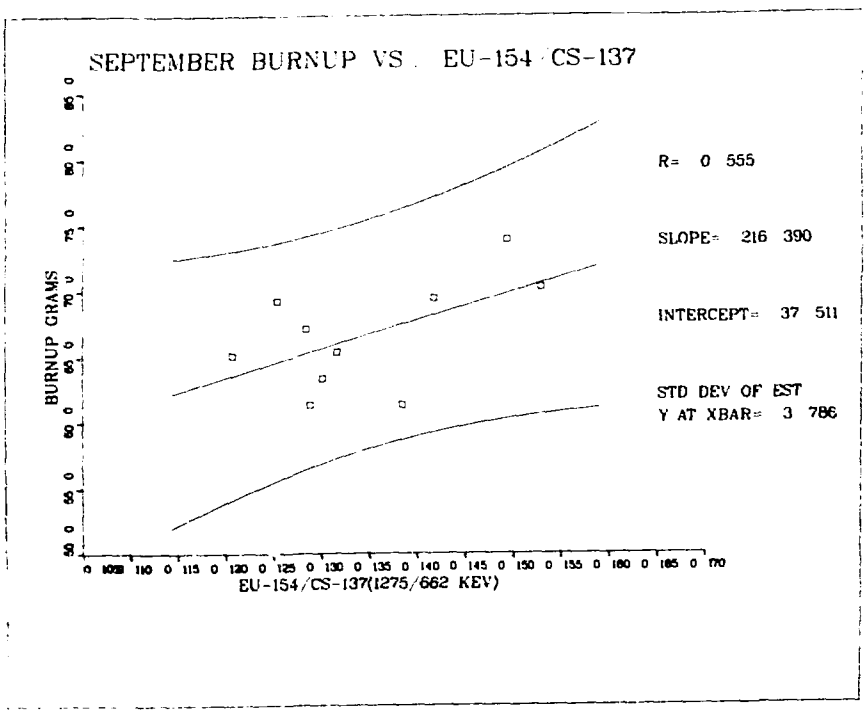

Fig. 12.

The linear relationship of declared burnup in grams with respect to ^{154}Eu (1275 keV)/^{137}Cs(662 keV) isotopic ratio.

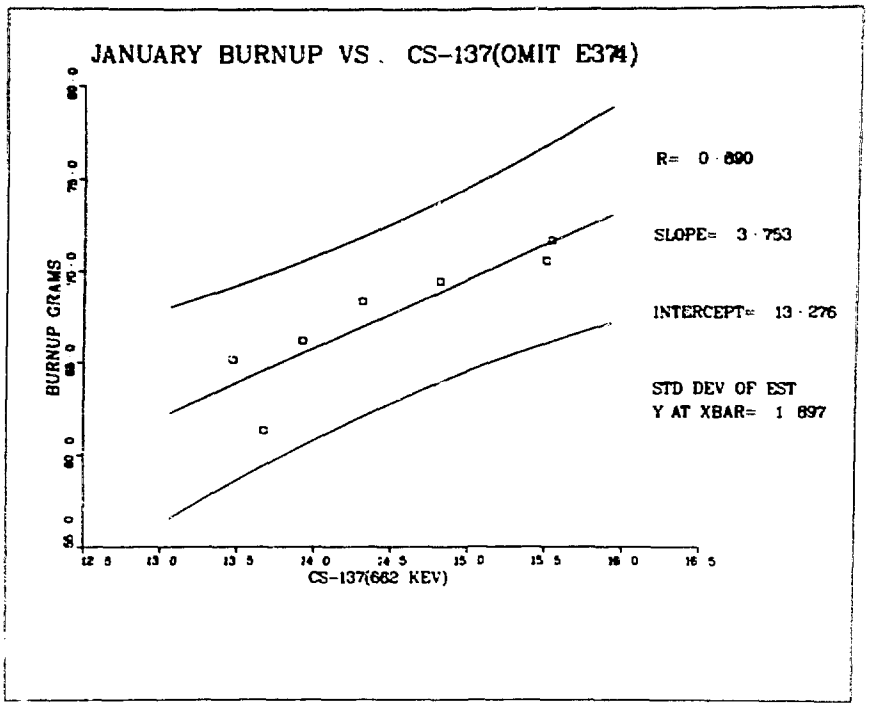

Fig. 13.
The linear relationship of declared burnup in grams with respect to ^{137}Cs (662 keV) activity for the January data.

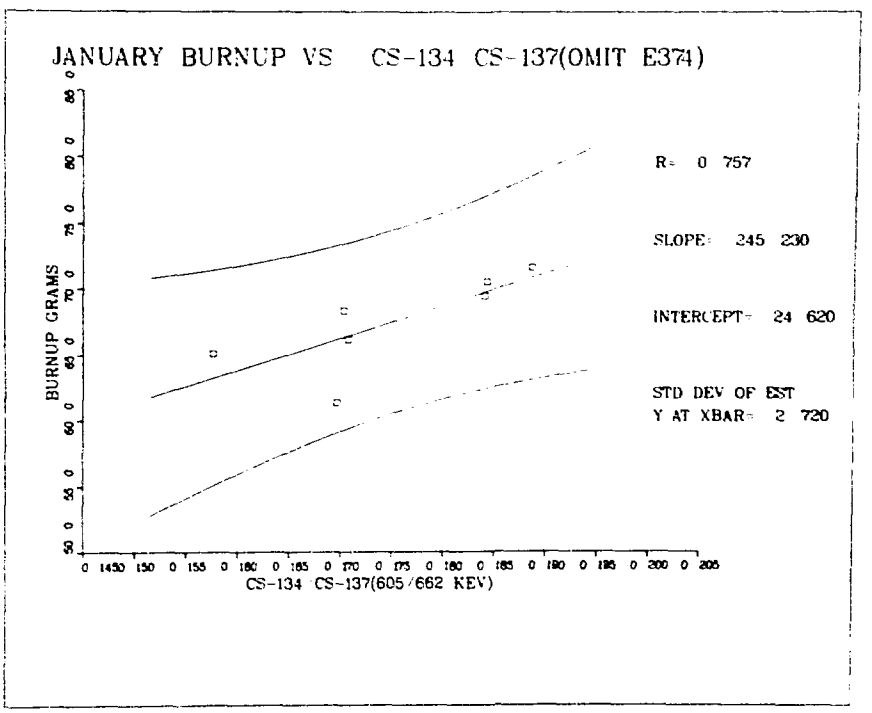

Fig. 14.
The linear relationship of declared burnup in grams with respect to ^{134}Cs (605 keV)/^{137}Cs(662 keV) isotopic ratio.

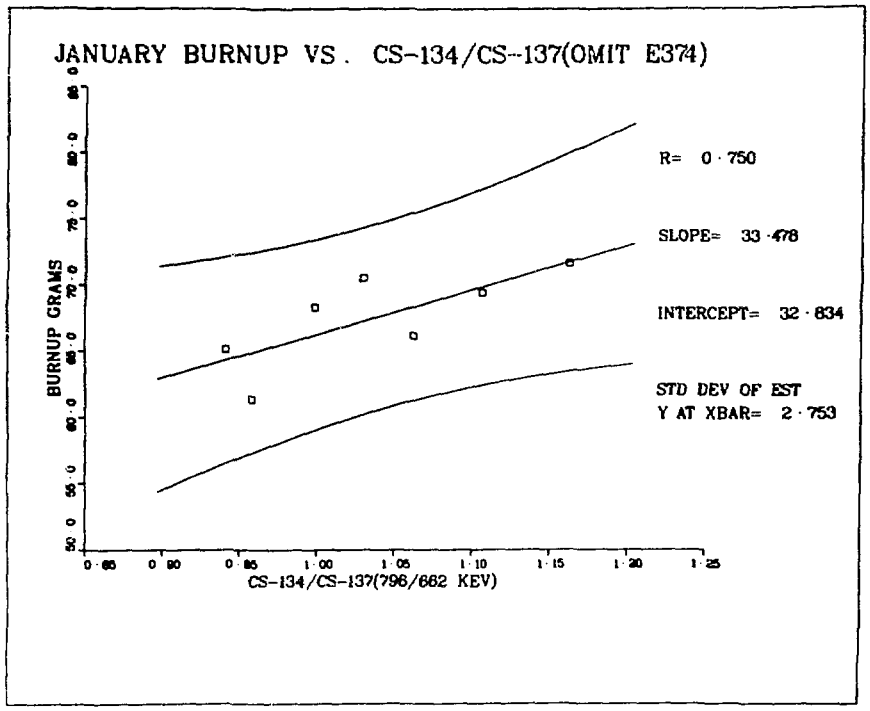

Fig. 15.

The linear relationship of declared burnup in grams with respect to ^{134}Cs (796 keV)/^{137}Cs(662 keV) isotopic ratio.

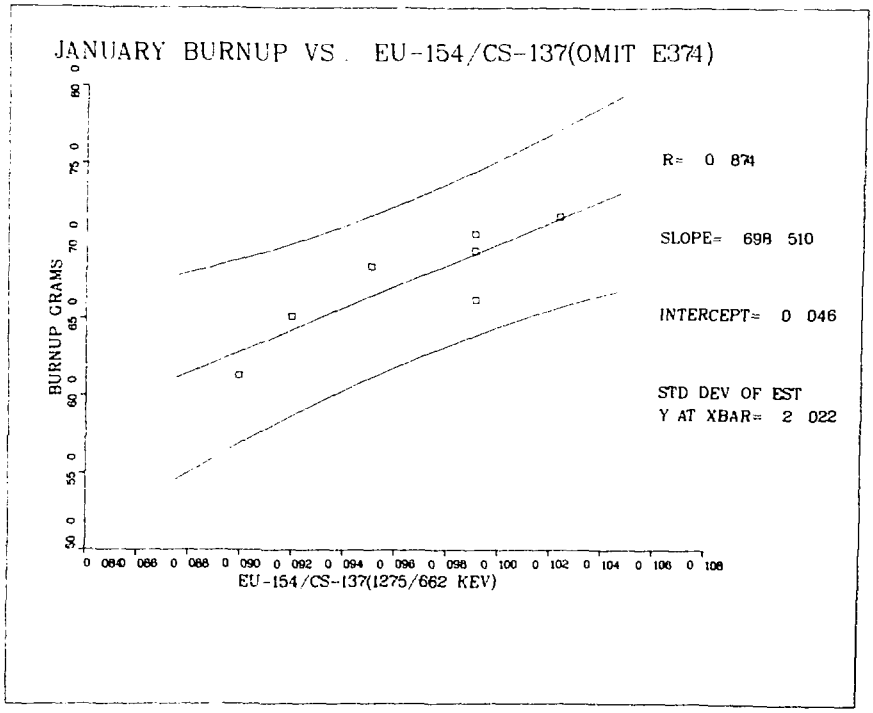

Fig. 16.

The linear relationship of declared burnup in grams with respect to ^{154}Eu (1275 keV)/^{137}Cs(662 keV) isotopic ratio.

TABLE IX

CONSISTENCY OF CALCULATED BURNUP VALUES BASED UPON FOUR PARAMETERS

	Element Identification											
September Data	E356	E359	E361	E363	E364	E368	E370	E371	E372	E378	% Variation Explained	Average Difference
Declared Value[3]	73.87	69.46	67.12	69.27	63.40	65.15	61.36	61.36	70.28	65.37		
Values Based on Regression Equation	74.11	71.43	66.33	67.20	63.81	63.63	62.73	63.70	67.04	66.13	80.3	2.2%
% Difference	+0.3	+2.8	-1.2	-3.0	+0.7	-2.3	+2.2	+3.8	-4.6	+1.2		

	Element Identification									
January Data	E357	E359	E368	E370	E373	E374[1]	E375	E379	% Variation Explained	Average Difference
Declared Value	71.64	69.46	65.15	61.36	70.54	65.65	68.38	66.22		
Values Based on Regression Equation	72.51	69.56	65.20	62.10	70.91	65.99	67.39	66.72	94.3	0.8%
% Difference	+1.2	+0.1	+0.1	+1.2	+0.5	-0.5	-1.5	+0.8		

---

1 Element E374 results are based upon its inclusion in the data analysis.

2 Measured values are based upon seven elements, with E374 excluded because of irregular irradiation exposure.

3 Burnup values are expressed in grams ^{235}U.

Both the $^{134}Cs/^{137}Cs$ and $^{154}Eu/^{137}Cs$ activity ratios involve an isotope which is produced via neutron capture reaction on a precursor fission product. The relationships of ^{134}Cs and ^{154}Eu with respect to ^{137}Cs were investigated by examining the data obtained in the axial profile measurements. The following functional relationship was evaluated

$$(^{134}Cs \text{ or } ^{154}Eu) = \alpha(^{137}Cs)^{\beta} \tag{13}$$

where ^{137}Cs is assumed to be directly proportional to the integrated flux and subsequently the burnup. The results from four assemblies are listed in Table X.

The data has been presented as a function of burnup in Fig. 17. The relationship appears to be a function of burnup with decreasing significantly as burnup increases. An exponent of 2.0 should be expected if ^{134}Cs and ^{154}Eu were proportional to flux squared, but the exponent for this set of data is generally significantly less than 2.0. If we assume that ^{137}Cs is proportional to flux and burnup is directly related to the integrated flux, then

$$\text{Burnup} \propto \frac{^{134}Cs}{^{137}Cs} \quad \text{where} \quad ^{134}Cs \propto (^{137}Cs)^{\beta}$$

$$\propto (^{137}Cs)^{\beta-1} \tag{14}$$

This would imply that burnup is not necessarily a linear function of either the $^{134}Cs/^{137}Cs$ or $^{154}Eu/^{137}Cs$ isotopic ratio, but rather a power function. The data obtained from the two $^{134}Cs/^{137}Cs$ ratios and the $^{154}Eu/^{137}Cs$ ratio have been corrected for this dependence and the burnup values recalculated in Table XI. The average differences show a general improvement over the values shown in Table VIII based upon uncorrected values for the isotopes.

Either the corrected or the uncorrected values could probably be used to measure the relative burnup of irradiated fuel assemblies over narrow ranges of burnup. However this may be a problem when measuring fuel assemblies with widely different burnups. The experimenter must be aware of this possible influence when interpreting the data.

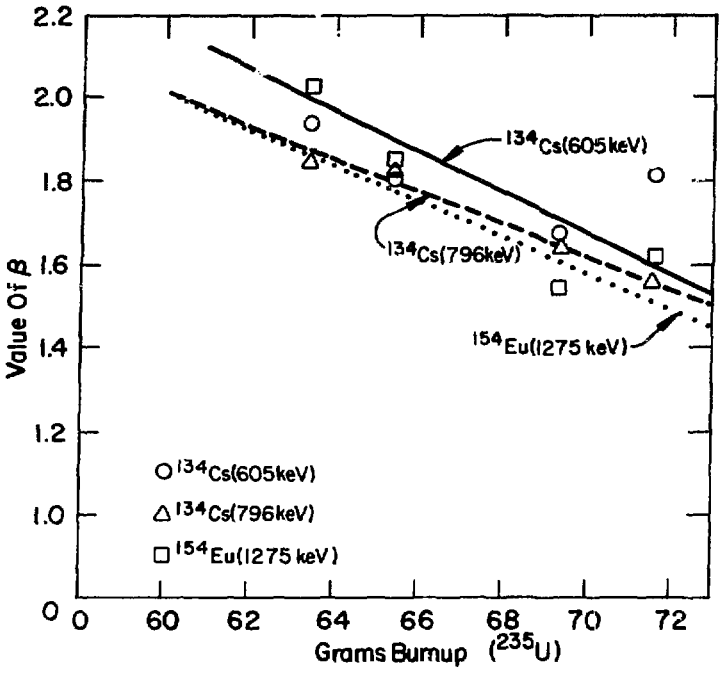

Fig. 17
β power factor as a function of declared burnup.

TABLE X

VALUES RELATING ^{134}Cs AND ^{154}Eu TO ^{137}Cs

Element	Declared Burnup, g	Power Factor - β $^{134}Cs(605)$	$^{134}Cs(796)$	$^{154}Eu(1275)$
383	63.37	1.94 ± 0.06	1.85 ± 0.07	2.03 ± 0.05
378	65.37	1.81 ± 0.05	1.82 ± 0.06	1.83 ± 0.15
363	69.27	1.67 ± 0.08	1.64 ± 0.07	1.54 ± 0.08
357	71.64	1.83 ± 0.18	1.56 ± 0.12	1.61 ± 0.18

IV. AXIAL PROFILE MEASUREMENTS

Four irradiated fuel elements were scanned axially using various nondestructive gamma-ray and neutron techniques to establish their axial burnup profiles. As was discussed previously, axial profile measurements are an integral part of any examination of irradiated fuel elements to ensure the integrity of the entire element and to provide a means of integrating burnup if the burnup is only measured at a single point. The axial distributions of ^{137}Cs were used as the standards for comparison.

TABLE XI

CALCULATED BURNUP VALUES BASED UPON CORRECTED ^{134}Cs AND ^{154}Eu VALUES

September Data

Element	Declared Burnup[1]	$^{134}Cs(605)/^{137}Cs(662)$	Difference	$^{134}Cs(796)/^{137}Cs(662)$	Difference	$^{154}Eu(1275)/^{137}Cs(662)$	Difference
357	71.64	73.29	2.3%	73.17	2.1%	72.92	1.8%
359	69.46	69.06	-0.6	69.16	-0.4	67.06	-3.5
368	65.15	65.27	0.2	64.78	-0.6	65.99	1.3
370	61.36	64.44	5.0	63.72	3.8	65.92	7.4
373	70.54	68.59	-2.8	68.88	-2.4	68.03	-3.6
374	65.65	65.07	-0.9	65.00	-1.0	66.00	0.5
375	68.38	67.06	-1.9	67.85	-0.8	66.42	-2.9
379	66.22	65.65	-0.9	65.84	-0.6	66.06	-0.2
			1.8%		1.5%		2.7%

January Data

356	73.87	75.97	2.8%	75.92	2.8%	74.29	0.6%
359	69.46	67.59	-2.7	67.90	-2.2	68.36	-1.6
361	67.12	65.71	-2.1	65.71	-2.1	64.88	-3.3
363	69.27	67.21	-3.0	67.29	-2.9	67.27	-2.9
364	63.46	64.38	1.4	64.28	1.3	64.02	0.9
368	65.15	64.87	-0.4	64.60	-0.8	64.20	-1.5
370	61.36	63.94	4.2	63.72	3.8	63.88	4.1
371	61.36	64.05	4.4	63.73	3.9	63.89	4.1
372	70.28	68.04	-3.2	68.62	-2.4	72.06	2.5
378	65.37	64.05	-0.6	64.94	-0.7	64.26	-1.7
			2.5%		2.3%		2.3%

[1] Burnup values are expressed in grams ^{235}U.

A. Germanium

Individual isotopes and isotopic ratios were correlated with the axial ^{137}Cs data obtained in the September and January exercises. Cluster analysis was used to separate the variables into general groups for further analysis. For each of the four elements the following variables appeared in a group: ^{134}Cs (605 keV), ^{134}Cs (796 keV), ^{137}Cs (662 keV), ^{134}Cs (796 keV)/ ^{144}Pr (2186 keV), ^{134}Cs (1365 keV)/^{144}Pr (2186 keV), and ^{134}Cs (796 keV)/ ^{106}Rh (1050 keV). Other variables appeared to be grouped for some elements, but change groups or do not fall into a specific group for all the other elements. The ^{134}Cs(605 keV)/^{137}Cs(662 keV) ratio distributions showed the highest degree of correlation with the ^{137}Cs axial activity.

The ^{134}Cs(605 keV)/^{137}Cs(662 keV) activity ratio explained at least 91% of the variation in the axial ^{137}Cs activity profile for each of the fuel elements. The data relating the $^{134}Cs/^{137}Cs$ ratio to ^{137}Cs activity for the axial scan of element E383 are presented in Fig. 18. The 95% confidence

bounds are plotted around the least squares functions. The standard deviation of the estimate of Y at x (mean) can be interpreted as the spread of one standard deviation (^{137}Cs activity) at the average measured value of ^{134}Cs/^{137}Cs.

B. Be(γ,n) Data

The axial profile of E383 was obtained using the Be(γ,n) detection assembly described in the Experimental section (Fig. 4) using various thicknesses of beryllium. Figure 19 shows the results obtained from a 2.5-and 5.0-cm thick beryllium converters with the small fission chamber surrounded with a 4-cm-polyethylene annulus. The comparison with the ^{137}Cs axial activity profile indicates that this type of detector could be used to measure the axial burnup profiles of irradiated MTR fuel elements. This detector is primarily sensitive to only the 2186 keV gamma emission of ^{144}Pr as the reaction threshold is 1660 keV for the production of a neutron. The fission chamber used to detect the neutrons is relatively insensitive to the gamma-ray background which can adversely affect other detection devices.

C. Cadmium Telluride Data

The cadmium telluride detector was also used to measure the axial gross gamma profile with disappointing results. Extremely high count rates, in excess of 100,000 counts/second, required the movement of the CdTe to distances of 0.3-0.6 meters from the fuel element to reduce saturation problems. Several attempts to shield the CdTe using 2.5-cm of lead and 1.0-cm tungsten were unsuccessful. Operation of the CdTe detector in the pulse mode appears to be limited to environments in which the count rate is less than 40,000 counts/second.

D. Fission Chamber Data

A large fission chamber with 1.6 g of ^{235}U was used to record the axial neutron profile of the E383 element. The MTR fuel was 93% enriched in ^{235}U so the spontaneous neutron emission rate from the higher transuranic isotopes (^{238}Pu, ^{240}Pu, ^{242}Cm, and ^{244}Cm) should be relatively low when compared to LWR assemblies. The maximum count rate with the fission chamber placed adjacent to the fuel element was only about 2 cpm. The results obtained from the neutron profile are plotted in Fig. 20 compared to the ^{137}Cs activity profile. Production of the spontaneous fissioning isotopes requires multiple neutron interactions, therefore, the 1/1.5 power of the fission chamber data gave the best fit. The actual power to which the fission chamber results must be raised for the best correlation to the actual burnup profile will depend

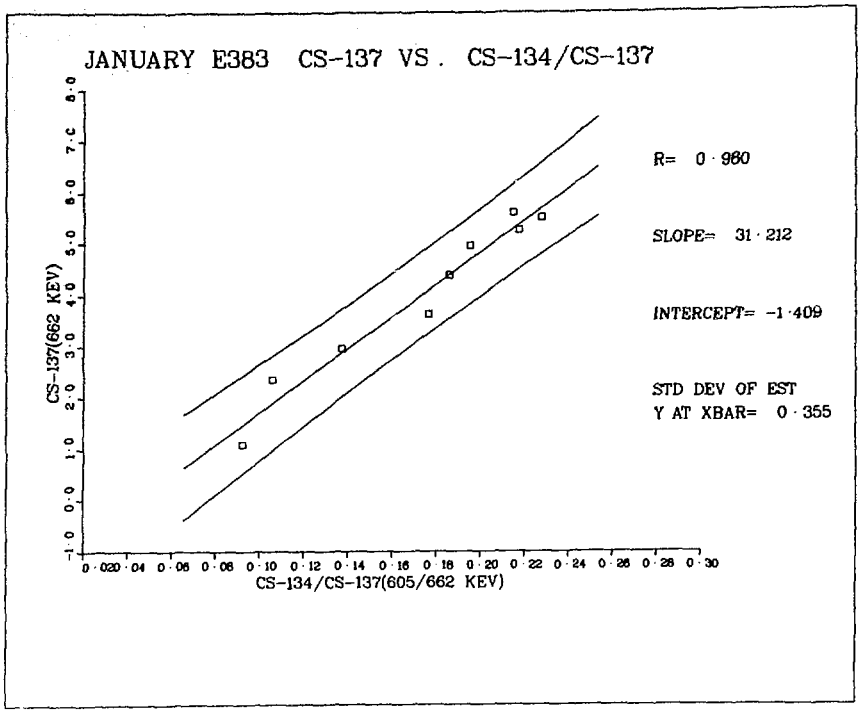

Fig. 18.
Comparison of the ^{134}Cs(605 keV)/ ^{137}Cs(662 keV) axial isotopic ratio for E383.

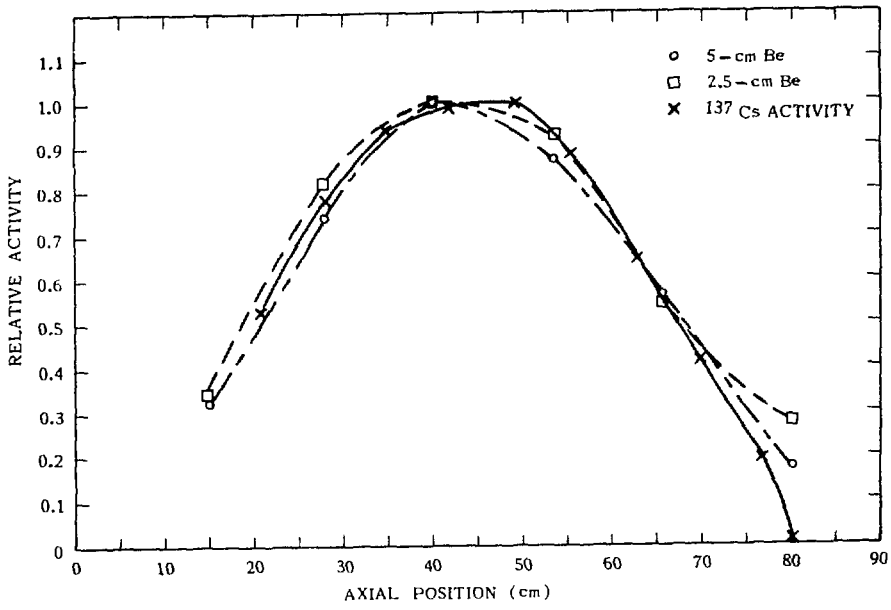

Fig. 19.
Axial plots of the Be(γ,n) detector with 2.5- and 5.0-cm of Be compared with the axial ^{137}Cs(662 keV) activity profile for E 383.

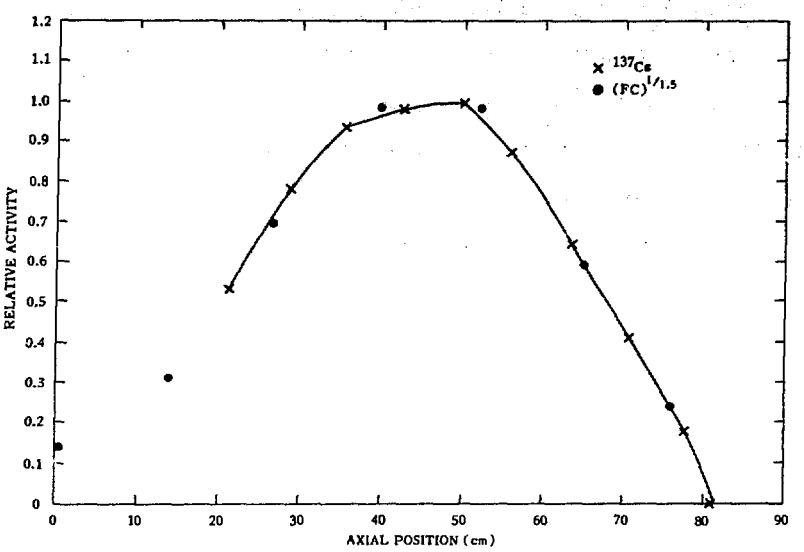

Fig. 20.
Comparison of ^{137}Cs axial profile with the neutron results raised to the 1/1.5 power.

upon the irradiation environment of the fuel element as well as the initial isotopic composition of the uranium. Also, the fission chamber is an uncollimated detector, that is, an extended detector looking at an extended source. These results should not be interpreted as quantitative but rather as an indication of the application of neutron techniques to profile and relative burnup measurement of irradiated fuel elements.

V. CONCLUSIONS

Various nondestructive gamma-ray and neutron techniques were applied to the characterization of the cooling times and burnups of irradiated MTR fuel elements. The correlation of all the major full-energy gamma-ray peaks and many isotopic ratios with these parameters were investigated using multivariate techniques to divide the number of independent variables into smaller groupings. Principal component analysis provided the number of dimensions required to contain most of the variations and cluster analysis provided a qualitative grouping of predictor variables. Both these statistical techniques were used to identify variables that should be investigated to quantify the prediction of relative cooling times and burnup values.

A nonlinear and linear model were investigated to represent the relationship between the measured variables and the declared cooling times. For the nonlinear model using known decay constants, the predicted values differed from the declared values by approximately 7% for single isotopes and by about 5% for isotopic ratios. By using regression analysis to calculate the coefficients the differences between predicted and declared values were reduced to about 4% for both single isotopes and isotopic ratios. In the nonlinear model the $^{144}Pr/^{137}Cs$ ratio consistently provided better prediction capability than any of the other isotopes or ratios. The half-life of ^{144}Ce, the parent of ^{144}Pr, is 284.4 days which is comparable to the cooling times measured. For shorter cooling times other isotopes (^{95}Zr; $t_{\frac{1}{2}}$=65.5 days, and ^{140}Ba-La: $t_{\frac{1}{2}}$=12.8 days) may be better predictors, similarly for longer cooling times $^{137}Cs(t_{\frac{1}{2}}=30.12\ y)$, $^{154}Eu(t_{\frac{1}{2}}=8.6\ y)$, and $^{134}Cs(t_{\frac{1}{2}}=2.06\ y)$ might have to be used. The ^{134}Cs and ^{154}Eu isotopes may be dependent upon the burnup of the fuel assemblies as was discussed in the axial profile section. In the linear model the independent variables, $^{134}Cs/^{137}Cs$ and $^{154}Eu/^{144}Pr$ exhibited the highest level of correlation for these ranges of cooling times.

The ^{137}Cs activity and three isotopic ratios, $^{134}Cs(605)/^{137}Cs(662)$, $^{134}Cs(796)/^{137}Cs(662)$, and $^{154}Eu(1275)/^{137}Cs(662)$, had the best correlations with the declared burnup values for both exercises. Using a linear combination of the four variables over 80% and 97% of the variations in the September and January data, respectively, could be explained using a linear model. The use of ratios or linear combinations as a consistency measurement is feasible with an uncertainty ranging from 2 to 4 grams for an average burnup value of 66 grams. This corresponds to a relative precision of 3-6% over the range of burnup values measured.

The functional relationships of the shielded isotopes ^{134}Cs and ^{154}Eu with respect to ^{137}Cs were shown to be a power function, with the exponent possibly being a function of burnup. Additional data will have to be analyzed before a definitive relationship can be established.

The axial burnup profile is required if we are to relate a single point measurement of burnup to the entire fuel element. A Be(γ,n) detector was used to measure the high-energy (>1.66 MeV) gamma profile of the irradiated elements. The high ^{235}U enrichment resulted in little buildup of even-numbered spontaneous fissioning isotopes within the fuel material. A fission chamber

monitored the axial neutron profile, which was a power relationship when correlated with the ^{137}Cs profile. Cadmium telluride detectors were of limited use in the pulse mode because of the very high gamma environments which saturated the detector.

The data obtained from these exercises will be used as input for the design and evaluation of similar measurements to be performed on light water reactor fuels. Similar statistical analyses will be applied to future data sets to determine consistency trends between measured variables and the important safeguard parameters: cooling times, axial profiles, and burnup values.

ACKNOWLEDGEMENTS

The assistance of the Omega West Reactor operations staff and particularly H. T. Williams and A. R. Lyle, was essential for the successful completion of this investigation. Mechanical support from L. R. Cowder, H. R. Dye, and D. C. Garcia in the construction and installation of the equipment was gratefully appreciated.

REFERENCES

1. "A Short History of Nonproliferation," International Atomic Energy Agency report IAEA-575 (February 1976).

2. Nucleonics Week, August 24, 1978 Vol. 19, No. 34, McGraw-Hill, New York.

3. S. T. Hsue, T. W. Crane, W. L. Talbert, Jr., J. C. Lee, "A Review of Nondestructive Assay Methods for Irradiated Nuclear Fuel," Los Alamos Scientific Laboratory report LA-6923 (December 1977).

4. T. Dragnev, R. Diaz-Duque, B. Pontes, "Safeguards Gamma Measurements on Spent MTR Fuel," International Atomic Energy Agency report IAEA/STR-41 (May 1973).

5. C. Beets, P. Bemelmans, T. Dragnev, R. Hecq, "Gamma Measurements on Spent Fuel Elements," ANS International Meeting, Safeguards and Nondestructive Assay Technology, Washington, D.C. (November 23, 1972).

6. G. L. Hanna, "Gamma-Ray Measurement of Spent HTFAR Fuel Elements for Safeguards Verification: Part I. Experimental Evaluation of Method," ASO/R2 (July 1978).

7. G. L. Hanna, "Gamma-Ray Measurement of Spent HTFAR Fuel Elements for Safeguards Verification: Part II. Theoretical Evaluation of Method," ASO/R2 (July 1978).

8. J. D. Chen, D. G. Bosge, R. B. Lypka, D. G. Zetaruk, "Nondestructive Determination of Burnup by Gamma Scanning: An Examination of $^{144}Ce/Pr$ and $^{134}Cs/^{137}Cs$ as Fission Monitors in CANDU Fuels," AECL report (1978).

9. J. Valovic, V. Petenyi, S. B. Rana, D. Mikusova, J. Kmosena, "The Application of Gamma and Isotopic Correlation Techniques for Safeguards Identification and Verification Purposes," International Atomic Energy Agency research contract 1443, Bohunice Nuclear Power Plant, Bohunice, Czechoslovakia (1975).

10. H. T. Williams, A. R. Lyle, O. W. Stopinski, C. L. Warner, Y. L. Yarnell, H. L. Maine, "1969 Status Report on the Omega West Reactor, with Revised Safety Analysis," Los Alamos Scientific Laboratory report LA-4192 (July 1969).

11. J. R. Beyster, L. A. Kull, "Safeguards Applications for Isotopic Neutron Sources," Brookhaven National Laboratory report BNL-50267 (T-596) (June 1970).

12. Chart of Nuclides, 12th Edition, Knolls Atomic Power Laboratory (April 1977).

13. N. R. Draper and H. Smith, Applied Regression Analysis, John Wiley and Sons, Inc., New York (1966).

14. D. F. Morrison, Multivariate Statistical Methods, McGraw-Hill, New York (1967).

15. P. H. A. Sneath and R. R. Sokel, Numerical Taxonomy, W. H. Freeman and Co., San Francisco (1973).

16. M. R. Anderberg, Cluster Analysis for Applications, Academic Press, New York (1973).

☆ U.S. Government Printing Office: 1979 – 677–013/153